XLVI CILAMCE
VITÓRIA - ES - BRAZIL - 2025
XLVI IBERO-LATIN AMERICAN CONGRESS ON COMPUTATIONAL METHODS IN ENGINEERING

Mechanical characterization and modeling of the skull of children affected by craniosynostosis

Brayan F. Pinzon G.[1], Jose A. Guerrero V.[2] , Maria C. Fukushima[1], Soraia Macari[3], Alexandre V. Gianetti[4], Estevam B. de las Casas[1].

[1]*School of Engineering, Federal University of Minas Gerais*
Av. Presidente Antônio Carlos, 6627 - Pampulha, 31270-901, Belo Horizonte - MG, Brazil
felipepinzon@gmail.com
[2]*School of Sciences and Engineering, Universidad del Rosario*
Calle 12c #6-25, Bogota D.C, Colombia
joseal.guerrero@urosario.edu.co
[3]*Department of Restorative Dentistry, Faculty of Dentistry, Federal University of Minas Gerais*
Av. Presidente Antônio Carlos, 6627 - Pampulha, 31270-901, Belo Horizonte - MG, Brazil
soraiamacari@gmail.com
[4]*Department of Surgery, Faculty of Medicine, Federal University of Minas Gerais*
Av. Prof. Alfredo Balena, 190 - Santa Efigênia 30130-100, Belo Horizonte - MG, Brazil
agjg@terra.com.br

Abstract. Sagittal craniosynostosis affects the normal development of the infant skull due to the premature fusion of the sagittal suture. This study proposes a methodology for the biomechanical modeling of the infant skull with sagittal craniosynostosis, focusing on the mechanical characterization of the cranial suture. To this end, two geometric models were developed: a simplified one to simulate three-point bending tests and another based on tomographic reconstruction of the complete skull. Through inverse analysis, the elastic modulus of the sagittal suture was estimated. In addition, simulations with different mechanical properties were performed using the finite element method to evaluate the effect of tissue stiffness on stress and deformation distribution. This methodology contributes to a better understanding of the biomechanical role of fused cranial sutures in bone development and lays the foundation for future studies with experimental validation and more advanced modeling.

Keywords: Biomechanics, finite element model, Sagittal craniosynostosis, suture.

1 Introduction

The human skull is composed of five main bones: two frontal bones, two parietal bones, and one occipital bone. These bones are responsible for protecting the brain and providing structural support to the head [1]. They are joined together by four sutures, which are anatomical structures made up of bands of fibrous connective tissue, and two fontanelles, which are membranous regions of soft tissue present during early development [2]. The sutures allow the ossification of the flat bones and enable the dynamic growth of the skull during the early years of life, acting as zones of controlled bone expansion. The fontanelles provide additional flexibility to the newborn's skull and gradually close as ossification progresses [3]. Brain development occurs in conjunction with skull growth, which is accelerated during the first years of a child's life. During this period, the sutures remain open to allow brain expansion and ensure an ideal intracranial volume [4]. Any alteration in this physiological process can compromise both the shape of the skull and the neurological function of the patient.

An atypical case occurs in about 1 in every 2,000 births, in which one or more sutures fuse prematurely, known as craniosynostosis, which is the second most common craniofacial anomaly [2][8]. This condition restricts normal skull growth and can result in morphological, physiological, and functional abnormalities; as well as cause intracranial hypertension, horizontal strabismus, cognitive deficits, and other neurological problems [4][8]. The most common type of craniosynostosis is scaphocephaly, which occurs when the sagittal suture fuses [5]. The

diagnosis of this condition is primarily made through clinical and imaging examinations, especially computed tomography scans (TC). The most common treatment is surgical intervention, which involves opening the affected suture and remodeling the skull. This procedure corrects deformities and prevents neurological consequences [7]. Due to the limited information available about this condition, different researches have been conducted over the past decade to expand knowledge about craniosynostosis. The goal of these investigations is to provide relevant information to clarify the origin of the condition and contribute to improving the treatments offered in medical centers [8], [9], [10].

Several studies have employed experimental and computational techniques to investigate cranial bones and sutures, providing valuable insights into the behavior of the infant skull. Experimentally, various authors have analyzed how changes in the speed and position of the three-point bending test affect the mechanical properties of both the parietal bone and the suture, concluding that these two parameters significantly influence the results obtained [9], [11]. Other studies conducted microstructural characterization of the parietal bone using nanoindentation, observing that the mechanical strength of infant bone is up to three times lower than that of adult bone [10], [12]. In terms of computational modeling, different investigations have used the finite element method to understand how the premature fusion of sutures affects skull development and shape, enabling the identification of regions with higher concentrations of stresses and strains [13], [14], [15]. Finally, the existing literature reveals a wide dispersion in the values of the mechanical properties of cranial tissues, which can be attributed to variations in age, sex, tissue type, and testing conditions [4], [16], [17], [18].

This study proposes a methodology for modeling the infant skull using a suture elastic modulus calculated from three-point bending tests of the bone suture bone interface reported in the literature [8], [9], under the assumption of Hookean behavior. To this end, two computational models were developed. The first was designed to determine the mechanical properties of the suture tissue through an inverse analysis using the finite element method. In the second analysis, both the elastic modulus obtained in the first simulation for the suture and the elastic modulus reported in the literature for the bones were employed to assess their influence on the biomechanical response of the finite element model. This approach allows for the analysis of the model's sensitivity to variations in suture stiffness and highlights the importance of accurate mechanical characterization. The following sections describe the methodology adopted for geometric reconstruction, material property assignment, and computational simulation, followed by the presentation of the main results and their discussion.

2 Methodology

2.1 Obtaining the Geometric Models

Two distinct geometric models were developed for the biomechanical study of craniosynostosis. The first model corresponds to a sample used in the three-point bending test from the study conducted by P. Swider et al. (2021) [18]. The geometry was created based on the dimensions reported for the central specimens of the stenotic sagittal suture (length: 30 mm, width: 6 mm, and thickness: 2.5 mm). This model was designed using Autodesk Inventor® software (Autodesk, California, USA) and consists of three differentiated layers: cortical bone, trabecular bone, and the sagittal suture. In this study, cortical and trabecular bone were distinguished with the aim that, in future research, this information will allow the independent analysis of each tissue's contribution to the elastic modulus. This model is shown in Figure 1A.

The second model corresponds to the tomographic reconstruction of the skull, sutures, and fontanelles, which was generated from a high-resolution computed tomography scan of an infant under one year of age diagnosed with sagittal craniosynostosis. The medical image processing was performed using Materialise Mimics and Materialise 3-Matic software (Materialise, Leuven, Belgium). In Mimics, the main anatomical structures were segmented: frontal, parietal, and occipital bones, as well as the sutures (metopic, coronal, and lambdoid). Due to the low mineralization of the sutures at this age, they could not be directly segmented. Therefore, 3-Matic software was used to manually reconstruct these tissues based on anatomical reference points derived from the visible bone contours. The final reconstruction model includes both fused and non-fused regions, allowing analysis of areas affected by synostosis as well as regions with normal physiological development. This reconstruction is shown in Figure 1B.

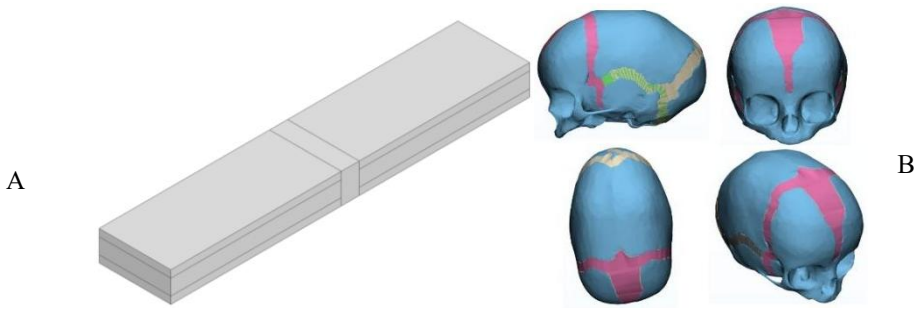


Figure 1. Geometric models. A. geometric model of the three-pint bending test, B. Reconstruction of a complete skull from a CT scan for the biomechanical analysis.

2.2 Numerical Simulation Using Finite Element Analysis

The finite element analysis was performed using Ansys Workbench 17.0 software (Ansys, Canonsburg, USA). Two independent simulations were developed, corresponding to the previously described geometric models.

For both models, bone and suture were modeled as linear, homogeneous, and isotropic materials [8], [10], [19] and the Poisson's ratio values were taken from the literature [17], [21]. For the first model, an effective elastic modulus of 940 MPa was used, as reported in the literature [18]. These values correspond to a sample composed of bone-suture-bone. Using these values and Euler-Bernoulli beam theory, a displacement of 0.919 mm was obtained, corresponding to the displacement measured in the three-point bending test. The general expression was rearranged to calculate the displacement, as shown below:

$$\delta = \frac{Fl^3}{4E_{EF}bh^3} \tag{1}$$

In this formulation, F represents the applied load, L the span length between supports, b the width of the sample, h its thickness, δ the displacement corresponding to the load F, and E the elastic modulus.

Subsequently, the proportion of the elastic modulus corresponding to cortical and trabecular bone was estimated. Since no studies explicitly reporting this distribution in multilayer models were found, a volume-based rule of mixtures was used to estimate the contribution of each material to the effective elastic modulus. Based on previous studies, it was assumed that the elastic modulus of trabecular bone is approximately 30% lower than that of cortical bone [20]. For the suture, a value of 30 MPa was assigned for the elastic modulus, according to reports in the literature on infant cranial connective tissue [4], [21]. The sample has a volume of 450 mm³, distributed as 205.2 mm³ of cortical bone (45.6% of the total volume), 222.3 mm³ of trabecular bone (49.4% of the total volume), and 22.5 mm³ of suture (5.0% of the total volume). These values were obtained through the geometry created in Autodesk Inventor. From this configuration, Equation 2 was solved to determine the elastic modulus of cortical and trabecular bone.

$$\begin{aligned} E_{EF} &= V_c * E_c + V_t * E_t + V_s * E_s \\ E_C &= \frac{E_{EF} - V_s * E_s}{V_c + 0.7 * V_t} \end{aligned} \tag{2}$$

In this equation, E_{EF} is the effective modulus, E_c is the elastic modulus of cortical bone, E_t is the elastic modulus of trabecular bone, E_s is the elastic modulus of the sagittal suture, V_c is the volume fraction of the cortical layer, V_t is the volume fraction of the trabecular layer, and V_s is the volume fraction of the sagittal suture.

Obtaining values of 1170.4 MPa for cortical bone and 819.3 MPa for trabecular bone, these were used as input data in the finite element simulation to obtain the directional displacement along the y-axis as output data. To reproduce the three-point bending test, two supports were employed: one with a fixed constraint and the other restricted only along the y-axis, in addition to a concentrated load of 12 N applied at the center of the geometry [18], as shown in Figure 2A. The displacement obtained in the simulation was compared with the displacement calculated using Equation 1, and inverse analysis was initiated. For this analysis, the elastic moduli of cortical and trabecular bone were kept fixed, while the elastic modulus of the suture was varied, since this tissue is the least rigid component and therefore has the greatest influence on the total deformation of the domain. This process was repeated until a value of the suture's elastic modulus was found that allowed the maximum displacement obtained through FEM to match the theoretically calculated displacement.

Four versions of the second model (complete skull) were created, varying the elastic modulus values of both the suture and the bone. For the first case, the material properties obtained from the first simulation were used. Since the geometry does not have a sandwich structure of cortical and trabecular bone, the volume-based rule of mixtures was used to obtain an average elastic modulus value for both tissues [18], employing Equation 3 and the same data presented earlier. The modulus obtained was 985.4 MPa. For the suture, the elastic modulus obtained through the inverse analysis method was used.

$$E_{prom} = \frac{V_c * E_c + V_t * E_t}{V_c + V_t} \tag{3}$$

For the other three versions, elastic modulus values for cortical bone, trabecular bone, and sagittal suture reported in the literature were used. This was done in order to assess the model's sensitivity to different mechanical properties. The values used are summarized Table 1.

Table 1. Mechanical properties obtained from literature sources for cranial tissues at different ages.

Simulation	Bone modulus [MPa]	Suture modulus [MPa]	Age group	Reference
Case 2	1103,01	408,12	1-2 years old	[11]
Case 3	783,8	4,2	11 months	[17]
Case 4	9870	1100	6 years old	[22]

For the boundary conditions, a fixed support was applied at the foramen magnum [23], and an intracranial pressure of 2660 Pa, simulating intracranial hypertension, was applied to the inner surface of the skull [24], [25], as shown in Figure 2B. To ensure the accuracy of the results, a convergence criterion based on the model's total deformation was employed. The mesh was progressively refined until the differences between successive solutions were less than 10% in terms of total deformation, resulting in a model composed of 544,107 nodes and 293,440 elements. In this simulation, total deformation and maximum stress were analyzed.

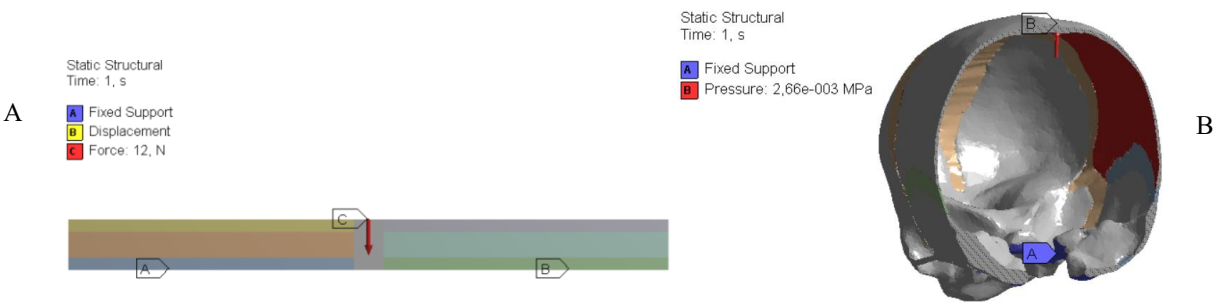


Figure 2. Boundary conditions, A. forces and constraints, first model, B. forces and constraints, second model.

3 Results

3.1 Numerical Simulation Using Finite Element Analysis

Through the iterations of the inverse analysis mentioned in the methodology, an elastic modulus of 61.2 MPa was obtained for the suture. Figure 3A shows the final simulation with the calculated theoretical displacement, and Figure 3B illustrates the evolution of the elastic modulus, the values are the deformations obtained with those Young's modulus. Additionally, the relative contribution of each tissue to the overall elastic modulus of the model was calculated. This analysis allowed quantifying how each component influences the total mechanical behavior of the system. The results showed that cortical bone contributes approximately 56.8% of the effective modulus, trabecular bone contributes 43%, and the sagittal suture represents only 0.2%.

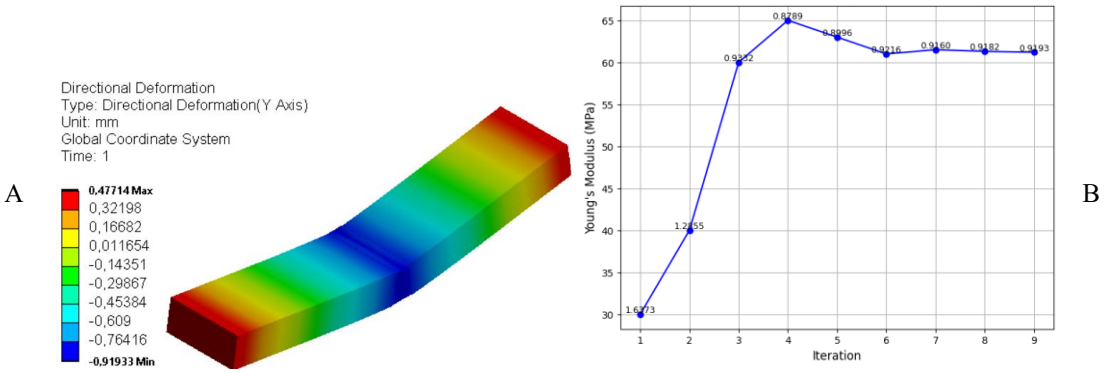


Figure 3. Convergence, A. Y-axis directional deformation, B. convergence to the calculated deformation.

For the second model, the results of total deformation and maximum principal stress obtained for the four simulated cases were as follows: in Case 1, the maximum total deformation was 0.05947 mm, located at the anterior fontanelle, while the maximum principal stress was 0.35912 MPa, found at the junction of the parietal bone and the right squamosal suture; in Case 2, the maximum total deformation was 0.03031 mm, located in the right parietal bone, and the maximum principal stress reached 0.31971 MPa, concentrated in the lower region of the same bone; in Case 3, the maximum total deformation was 0.30373 mm, located at the anterior fontanelle and at the junction of the parietal bone with the left squamosal suture, while the maximum principal stress was 0.44194 MPa, located at the junction of the parietal bone and the right squamosal suture; and Case 4 showed the lowest total deformation, with a value of 0.0047432 mm at the anterior fontanelle, and the maximum principal stress was 0.34176 MPa, located at the junction of the parietal bone and the squamosal suture. Figure 4 presents the final simulation results for each of the four cases, as well as for each of the analyzed variables.

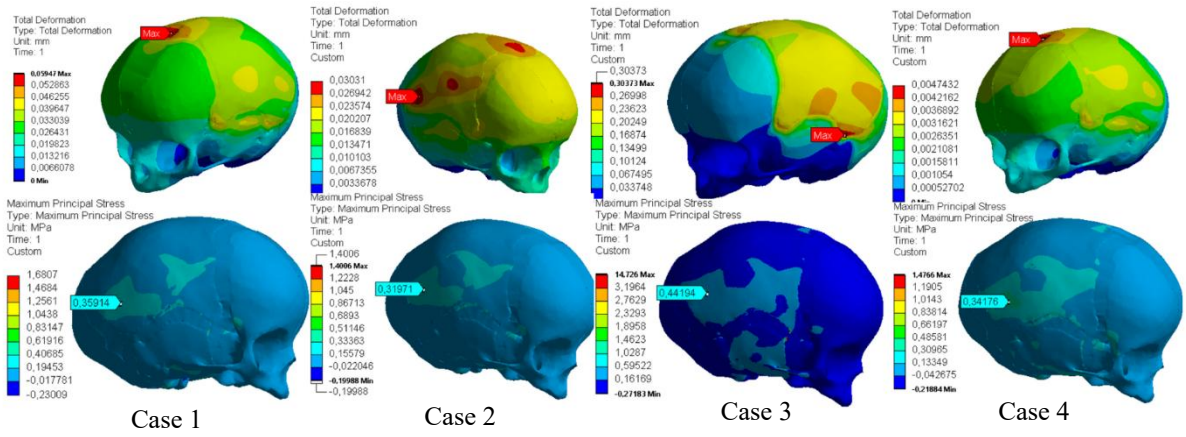


Figure 4. Comparison of Maximum Deformation and Stress per Simulation Case

4 Discussion

The results obtained through numerical simulation provide insight into how tissue mechanical characterization influences the biomechanical behavior of the infant skull with craniosynostosis, both in terms of deformation and stress distribution. This was evidenced by the variation in the elastic modulus of the different tissues composing the geometry.

In the first model, the iterative adjustment of the effective elastic modulus made it possible to reproduce the central displacement of 0.919 mm, which corresponded to an effective modulus of 940 MPa. The elastic modulus results for cortical and trabecular bone align with literature reports, where the elastic modulus of infant cortical bone shows greater stiffness compared to trabecular bone [4], [12], [26].

Additionally, it was found that the elastic modulus of the suture is 61.2 MPa, a value that falls within the

ranges reported in other studies [11], [18]. It is noteworthy that, in this model, the suture represented only 5% of the total sample volume, and its contribution to the effective modulus was just 0.2%. This highlights the relatively low stiffness of this tissue compared to the surrounding bone, reinforcing its role as a biomechanical transition zone.

In Cases 1 and 3, where the elastic moduli of both bone and suture were lower, it was observed that the maximum deformations occurred in the anterior fontanelle, with a wider distribution of stresses in the junction regions between bone and suture. This is consistent with studies that conclude that open sutures act as mechanical damping zones, capable of absorbing energy and reducing the load on adjacent bones [27].

On the other hand, in Cases 2 and 4, which had higher stiffness in their mechanical properties, the models tended to concentrate stresses in specific bone connection areas, with smaller and more localized deformations. However, it was noted that the maximum principal stress did not decrease proportionally with the increase in stiffness, demonstrating that greater stiffness does not guarantee a reduction in stress nor does it lead to a more favorable load distribution [28].

In all cases, it was observed that both the anterior fontanelle and the junction of the parietal bone with the squamosal suture act as stress concentrators, supporting the hypothesis that sagittal craniosynostosis significantly alters the internal distribution of stress. This is because the premature fusion of the sagittal suture severely restricts perpendicular skull growth, preventing uniform brain expansion. These findings are consistent with other studies using FEM [29], [30], [31]. Finally, the analysis of the suture showed that this tissue has a strong impact on the final morphology of the skull, as fused (stiffer) sutures generate higher stresses, which explains the deformations characteristic of this condition.

5 Conclusion

The present study demonstrated that the methodology used to determine the elastic modulus of the suture is valid. Regarding the results, it was observed that variations in the elastic modulus of the tissues that compose the skull significantly influence deformation patterns and stress distribution in infant skulls with sagittal craniosynostosis. Although sutures are the least predominant tissue in the skull, they play a fundamental role in the redistribution of mechanical loads. It was found that a model with higher stiffness leads to localized stress concentrations, whereas lower mechanical properties allow for greater deformation and better stress dissipation. These results highlight the importance of accurately characterizing the mechanical behavior of sutures, suggesting the need for further mechanical testing that takes into account variables such as the type of craniosynostosis and other morphological characteristics.

6 References

[1] M. S. Raam, B. D. Solomon, S. A. Shalev, y M. Muenke, «Holoprosencephaly and craniosynostosis: A report of two siblings and review of the literature», *Am. J. Med. Genet.*, vol. 154C, n.º 1, pp. 176-182, feb. 2010, doi: 10.1002/ajmg.c.30234.

[2] L. Ibarra *et al.*, «Guía clínica: alteraciones de la forma del cráneo», *Archivos de Pediatría del Uruguay*, 2022.

[3] D. A. Garzón-Alvarado, «A hypothesis on the formation of the primary ossification centers in the membranous neurocranium: A mathematical and computational model», *Journal of Theoretical Biology*, vol. 317, pp. 366-376, ene. 2013, doi: 10.1016/j.jtbi.2012.09.015.

[4] S. S. Margulies y K. L. Thibault, «Infant Skull and Suture Properties: Measurements and Implications for Mechanisms of Pediatric Brain Injury», *Journal of Biomechanical Engineering*, vol. 122, n.º 4, pp. 364-371, ago. 2000, doi: 10.1115/1.1287160.

[5] M. Geoffroy, P.-M. François, R. H. Khonsari, y S. Laporte, «Paediatric skull growth models: A systematic review of applications to normal skulls and craniosynostoses», *Journal of Stomatology, Oral and Maxillofacial Surgery*, vol. 123, n.º 5, pp. e533-e543, oct. 2022, doi: 10.1016/j.jormas.2022.01.002.

[6] M. Turgut, R. S. Tubbs, A. T. Turgut, y A. S. Dumont, Eds., *The Sutures of the Skull: Anatomy, Embryology, Imaging, and Surgery*. Cham: Springer International Publishing, 2021. doi: 10.1007/978-3-030-72338-5.

[7] J. M. González Darde, «Historia de la craneotomía», *Neurocirugía*, vol. 27, n.º 5, pp. 245-257, sep. 2016, doi: 10.1016/j.neucir.2016.02.002.

[8] B. J. Igo, P. S. Cottler, J. S. Black, y M. B. Panzer, «The mechanical and microstructural properties of the pediatric skull», *Journal of the Mechanical Behavior of Biomedical Materials*, vol. 120, p. 104578, ago. 2021, doi: 10.1016/j.jmbbm.2021.104578.

[9] J. A. Motherway, P. Verschueren, G. Van Der Perre, J. Vander Sloten, y M. D. Gilchrist, «The mechanical properties of cranial bone: The effect of loading rate and cranial sampling position», *Journal of Biomechanics*, vol. 42, n.º 13, pp. 2129-2135, sep. 2009, doi: 10.1016/j.jbiomech.2009.05.030.

[10] J.-W. Wang *et al.*, «Application of nanoindentation technology in testing the mechanical properties of skull materials», *Sci Rep*, vol. 12, n.º 1, p. 8717, may 2022, doi: 10.1038/s41598-022-11216-6.

[11] Y. Chen, «Mechanical Properties of Cranial Bones and Sutures in 1–2-Year-Old Infants», *Med Sci Monit*, vol. 20, pp. 1808-1813, 2014, doi: 10.12659/MSM.892278.

[12] S. Ajami *et al.*, «Mechanical and morphological properties of parietal bone in patients with sagittal craniosynostosis», *Journal of the Mechanical Behavior of Biomedical Materials*, vol. 125, p. 104929, ene. 2022, doi: 10.1016/j.jmbbm.2021.104929.

[13] A. Borghi *et al.*, «Spring assisted cranioplasty: A patient specific computational model», *Medical Engineering & Physics*, vol. 53, pp. 58-65, mar. 2018, doi: 10.1016/j.medengphy.2018.01.001.

[14] W. Wolański, D. Larysz, M. Gzik, y E. Kawlewska, «Modeling and biomechanical analysis of craniosynostosis correction with the use of finite element method: MODELING AND BIOMECHANICAL ANALYSIS OF CRANIOSYNOSTOSIS CORRECTION», *Int. J. Numer. Meth. Biomed. Engng.*, vol. 29, n.º 9, pp. 916-925, sep. 2013, doi: 10.1002/cnm.2506.

[15] G. Zhang *et al.*, «A Systematic Approach to Predicting Spring Force for Sagittal Craniosynostosis Surgery», *Journal of Craniofacial Surgery*, vol. 27, n.º 3, pp. 636-643, may 2016, doi: 10.1097/SCS.0000000000002590.

[16] P. Verschueren, H. Delye, D. Berckmans, I. Verpoest, J. Goffin, y J. V. Sloten, «Analysis of Fracture Characteristics of Cranial Bone for FE Modelling», 2006.

[17] B. Coats y S. S. Margulies, «Material Properties of Human Infant Skull and Suture at High Rates», *Journal of Neurotrauma*, vol. 23, n.º 8, pp. 1222-1232, ago. 2006, doi: 10.1089/neu.2006.23.1222.

[18] P. Swider *et al.*, «Mechanical properties of fused sagittal sutures in scaphocephaly», *Clinical Biomechanics*, vol. 86, p. 105369, jun. 2021, doi: 10.1016/j.clinbiomech.2021.105369.

[19] O. Malde, J. Libby, y M. Moazen, «An Overview of Modelling Craniosynostosis Using the Finite Element Method», *Mol Syndromol*, vol. 10, n.º 1-2, pp. 74-82, 2019, doi: 10.1159/000490833.

[20] J. Y. Rho, R. B. Ashman, y C. H. Turner, «Young's modulus of trabecular and cortical bone material: Ultrasonic and microtensile measurements», *Journal of Biomechanics*, vol. 26, n.º 2, pp. 111-119, feb. 1993, doi: 10.1016/0021-9290(93)90042-D.

[21] M. Moazen, E. Peskett, C. Babbs, E. Pauws, y M. J. Fagan, «Mechanical Properties of Calvarial Bones in a Mouse Model for Craniosynostosis», *PLoS ONE*, vol. 10, n.º 5, p. e0125757, may 2015, doi: 10.1371/journal.pone.0125757.

[22] M. T. Davis *et al.*, «The mechanical and morphological properties of 6 year-old cranial bone», *Journal of Biomechanics*, vol. 45, n.º 15, pp. 2493-2498, oct. 2012, doi: 10.1016/j.jbiomech.2012.07.001.

[23] X. Li, H. Sandler, y S. Kleiven, «The importance of nonlinear tissue modelling in finite element simulations of infant head impacts», *Biomech Model Mechanobiol*, vol. 16, n.º 3, pp. 823-840, jun. 2017, doi: 10.1007/s10237-016-0855-5.

[24] T. Nagasao *et al.*, «A Biomechanical Study on the Effect of Premature Fusion of the Frontosphenoidal Suture on Orbit Asymmetry in Unilateral Coronal Synostosis», *The Cleft Palate-Craniofacial Journal*, vol. 47, n.º 1, pp. 82-91, ene. 2010, doi: 10.1597/08-164.1.

[25] M. Harary, R. G. F. Dolmans, y W. B. Gormley, «Intracranial Pressure Monitoring—Review and Avenues for Development», *Sensors*, vol. 18, n.º 2, p. 465, feb. 2018, doi: 10.3390/s18020465.

[26] G. K. McPherson y T. J. Kriewall, «The elastic modulus of fetal cranial bone: A first step towards an understanding of the biomechanics of fetal head molding», *Journal of Biomechanics*, vol. 13, n.º 1, pp. 9-16, ene. 1980, doi: 10.1016/0021-9290(80)90003-2.

[27] Q. Wang *et al.*, «The Role of the Sutures in Biomechanical Dynamic Simulation of a Macaque Cranial Finite Element Model: Implications for the Evolution of Craniofacial Form», *The Anatomical Record*, vol. 295, n.º 2, pp. 278-288, feb. 2012, doi: 10.1002/ar.21532.

[28] Q. Wang *et al.*, «The Global Impact of Sutures Assessed in a Finite Element Model of a Macaque Cranium», *The Anatomical Record*, vol. 293, n.º 9, pp. 1477-1491, sep. 2010, doi: 10.1002/ar.21203.

[29] F. J. Burgos-Flórez y D. A. Garzón-Alvarado, «Stress and strain propagation on infant skull from impact loads during falls: a finite element analysis», *International Biomechanics*, vol. 7, n.º 1, pp. 19-34, ene. 2020, doi: 10.1080/23335432.2020.1719196.

[30] C. Cross, R. H. Khonsari, D. Larysz, D. Johnson, L. Kölby, y M. Moazen, «Predicting and comparing three corrective techniques for sagittal craniosynostosis», *Sci Rep*, vol. 11, n.º 1, p. 21216, oct. 2021, doi: 10.1038/s41598-021-00642-7.

[31] C. Cross *et al.*, «Using Sensitivity Analysis to Develop a Validated Computational Model of Post-operative Calvarial Growth in Sagittal Craniosynostosis», *Front. Cell Dev. Biol.*, vol. 9, p. 621249, may 2021, doi: 10.3389/fcell.2021.621249.